chemistry

MDPI

Article

Ratiometric Fluorescent Detection of Carbaryl Based on Molecular Intrinsic Fluorescence Enhancement and Gold Nanoclusters

Xiujin Chen [1,*], Jingyang Jiang [2], Xiufang Huang [2] and Chifang Peng [2,*]

[1] College of Food and Bioengineering, Henan University of Science and Technology, Luoyang 471000, China
[2] School of Food Science and Technology, Jiangnan University, Lihu Road 1800, Wuxi 214122, China
* Correspondence: chenxiujin9610@126.com (X.C.); pcf@jiangnan.edu.cn (C.P.)

Abstract

In this work, a ratiometric fluorescent method for carbaryl detection is reported. We found that the combination of rapid hydrolysis of carbaryl and cetyltrimethylammonium bromide (CTAB) emulsification could significantly enhance the intrinsic weak blue fluorescence of carbaryl. By using red fluorescent glutathione-gold nanoculsters (GSH-Au NCs) as a reference signal, ratiometric detection of carbaryl within 3 min was successfully achieved. The method exhibited high sensitivity, with a linear response to carbaryl in the range from 1.0 to 70 ng/mL and an LOD of 0.05 ng/mL. The method was applied for detection of carbaryl in apple and cabbage samples, and recovery rates of 90~101% and 93~110%, respectively, were obtained. These results show that the proposed method for carbaryl detection has great potential for application in food sample monitoring.

Keywords: carbaryl; fluorescence; enhancement; ratiometric detection

1. Introduction

Carbaryl (1-Naphthol methylcarbamate), a type of carbamate insecticide with high activity and a broad-spectrum effect, is widely used for the control of diseases affecting beans, vegetables and fruit trees [1,2]. However, carbaryl residues not only harm the environment, but also are highly toxic to human beings through skin contact and respiratory transmission [3]. European regulations state that carbaryl should be limited to between 0.01 mg/kg and 0.5 mg/kg in agricultural products [4]. Therefore, there is an increasingly need to develop a sensitive detection method for carbaryl.

Many methods have been reported for detection of carbaryl, such as chromatography [5], enzyme-linked immunosorbent assay [6] and electrochemical assay [7]. However, these methods are relatively complicated and expensive, or they may require skilled operators, greatly limiting their practical applications. In the pursuit of cost-effective methods, the enzyme-activity-inhibiting effects of pesticides upon acetylcholinesterase (AchE) have been explored. For example, Li et al. proposed that the AchE hydrolysate thiocholine could decompose a "T-Hg^{2+}-T" formation originating from a helper DNA probe, and quench a fluorophore probe output fluorescent signal. In [8], in the presence of a carbamate pesticide, AchE activity was inhibited and the fluorescence signal was quenched. Korram et al. reported a method based on the FRET effect, with carbon dots (CDs) as donor and AuNPs as acceptor. Detection was achieved by measuring the turn-on fluorescence signal of CDs in the presence of carbamate pesticide due to inhibition of the

Academic Editor: Haishi Cao

Received: 26 January 2026
Revised: 17 March 2026
Accepted: 18 March 2026
Published: 19 March 2026

catalytic activity of AchE [9]. Some fluorescent-nanomaterial-based chemosensors have also demonstrated good performance in pesticide detection [10]. Khaledian et al. reported on synthesis of a CD probe and detection of the organophosphorus pesticide diazinon based on the quenching effect of fluorescence [11]. Shen et al. fabricated a fluorescence probe $[Ru(bpy)_3]^{2+}$-functionalized liposome-encapsulated curcumin ($[Ru(bpy)_3]^{2+}$@CCM-NPs) through electrostatic interaction. On the basis of the fluorescence quench effect of ClO^- upon curcumin and the fluorescence of $[Ru(bpy)_3]^{2+}$, they constructed a ratiometric fluorescence system and achieved accurate on-site detection of ClO^- [12]. Chen et al. synthesized novel Flavourzyme-stabilized gold nanoclusters (Fla-Au NPCs) which showed evident fluorescent enhancement by carbaryl, and then successfully sensed carbaryl [2].

Although the above fluorescent methods for sensing carbaryl are now well established, these methods strongly depend on the interaction between carbaryl and the surface ligand of fluorescent nanomaterials. Another method involves seeking the intrinsic fluorescent characters of pesticides. However, the intrinsic fluorescence emission of pesticides is commonly very weak, and this is difficult to apply in sensing. To achieve fluorescence-turn-on sensing of targets, researchers have deeply investigated environmental factors such as surfactants, micelles, solution environments, and supermolecular compounds. Liu et al. described a method using Triton X-100 as an assisted surfactant to construct an amplified-fluorescence detection strategy for Pd^{2+} [13]. Li et al. reported that addition of cetyltrimethylammonium bromide (CTAB) can effect electrostatic interaction between negatively charged CDs, causing self-aggregation and enhancing the quantum yield [14]. Du et al. found that in the presence of the deblock copolymer PEG-PLLA, a 1,1′-bi-2-Naphthol(BINOL)-based fluorescence probe could be encapsulated into micelle and exhibit fluorescence enhancement, so that detection of L- and D-tryptophan could be achieved [15]. Oh et al. reported that a tryptophan-based fluorescent probe could be encapsulated into SDS micelles, resulting in significant enhancement of red emission [16]. Hu et al. reported that a new intramolecular charge transfer (ICT) compound (E)-2-(((2-hydroxynaphthalen-1-yl)methylene)amino) benzoic acid (HABA) showed greatly enhanced fluorescence in polar protic solvent [17]. Li et al. synthesized a rhodamine B-benzofurazan-based fluorescence probe which showed greatly enhanced fluorescence in aqueous solution containing 30% ethanol [18]. Azath et al. reported a composite fluorescence probe based on 7-Aminoflavone-modified cyclodextrin which could enhance fluorescence and thus achieve detection of Cu^{2+} [19]. Tang et al. reported a supermolecular fluorescent probe Proflavine @ cucurbit [8] uril (2PF@Q [8]) showed remarkable fluorescence enhancement with l-borneol [20].

Under alkaline condition, carbaryl can be easily hydrolyzed to 1-naphthol, which is strongly hydrophobic and exhibits weak blue fluorescence. In light of the fact that a surfactant can encapsulate and assist the dissolution of hydrophobic molecules, thus protecting the quenching of molecular fluorescence by water molecules [13–15], in this work, for the first time, we utilized CTAB as a fluorescence enhancer of carbaryl hydrolysate, and also introduced GSH-templated Au NCs as a ratiometric reference signal. By such means, a highly sensitive ratiometric fluorescent detection of carbaryl was achieved. In addition, the proposed method could be completed within 3 min, and it was successfully applied for the detection of food samples.

2. Experimental Section

2.1. Materials and Apparatus

All chemicals were used directly without any further purification, and all chemical reagents in this experiment were analytical-grade. Chlorauric acid ($HAuCl_4$) and glutathione (GSH) were purchased from Shanghai Sinopharm Reagent Co. Cetyltrimethylam-

monium bromide (CTAB) was bought from Shanghai Aladdin Biochemical Technology Co. (Shanghai, China). All experimental water resistance values were higher than 18 MΩ/cm.

Fluorescence spectra were recorded through a UV-2802 pcs ultraviolet spectrophotometer and an F97 Pro fluorescence spectrophotometer (Shanghai Ling Guang Technology Co., Ltd., Shanghai, China). The transmission electron microscope (TEM) images of DNA-Ag NCs were obtained using a JEOL-2100 transmission electron microscope (Japan Electron Optics Laboratory CO., Ltd., Tokyo, Japan). Measurement and management of material was completed using an AUY-120 electronic balance (MS105DU, Mettler Toledo Instruments Shanghai Co., Ltd., Shanghai, China).

2.2. Preparation of GSH-Au NCs

Synthesis of GSH-Au NCs was based on a previously reported procedure with a minor modification [21]: 2 mL $HAuCl_4$ (10 mM) was added to 8 mL GSH solution (3.75 mM) with vigorous stirring at 25 °C. After the color of the solution changed from yellow to brown, it was stored at 70 °C for 24 h, then cooled to room temperature. Finally, the solution was stored at 4 °C for future use.

2.3. Fluorescence Detection of Carbaryl

The standard carbaryl substance was dissolved in methanol to 1 mg/mL and diluted with deionized water to prepare a series of solutions at different concentrations. Next, 10 μL amounts of carbaryl solution at different concentrations were mixed with 10 μL of NaOH (100 mM) and 20 μL of CTAB (50 mM) and allowed to react for 3 min at room temperature. The final volume was adjusted to 100 μL with 50 μL deionized water and 10 μL diluted GSH-Au NCs (50×). The fluorescent-emission spectra were recorded for carbaryl detection.

2.4. Pretreatment and Carbaryl Detection of Food Samples

Apples and cabbages were bought from a supermarket and used as real samples in this experiment. First, 20 mL of carbaryl (0.2 ng/mL, 0.6 ng/mL, 1.2 ng/mL) was added to 1 g of apple or cabbage. After the spiked samples (4.0, 12.0 and 24.0 ng/g) had been allowed to stand for 1 h, they were homogenized. Mixtures were then centrifuged at 5000 rpm for 10 min. Finally, the collected supernatants were filtered through a 0.22 μm filter; fluorescence emission spectra were then recorded as described above, and recovery rates were calculated.

3. Results and Discussion

3.1. Feasibility of Carbaryl Sensing

The principle of the proposed method for carbaryl detection is illustrated in Figure 1. Under an alkaline environment, carbaryl is mainly hydrolyzed into 1-naphthol. This is because the methyl isocyanate group of carbaryl is attacked by hydroxide ions through a SN_2 substitution reaction [22,23] and the intermediate methyl isocyanate ($CH_3N{=}C{=}O$) is unstable and easily hydrolyzed to CO_2 and methylamine [24]. Under excitation of 350 nm, 1-naphthol exhibited weak blue fluorescence which could be greatly enhanced by CTAB, one of the cationic surfactants. GSH-Au NCs are biocompatible and exhibit a high quantum yield [25]. These remained relatively stable and showed obvious red fluorescence at 620 nm under both alkaline and high-concentration-of-CTAB conditions. The cationic surfactant CTAB and the negatively charged GSH could be bonded through electrostatic interaction, which could improve the stability of the sensing system. The mixture of carbaryl hydrolysate and GSH-Au NCs showed two fluorescence emission peaks under excitation of 350 nm. With the introduction of carbaryl, the blue fluorescence emission at 450 nm increased, and the fluorescence emission at 620 nm remained stable.

The GSH-Au NCs could therefore be used to output a reliable reference signal. Ratiometric fluorescent detection is a very popular sensing mode which has attracted great interest from many researchers [7]. This design of ratiometric fluorescent detection could help promote resistance to environmental interference and achieve visualization of the detection.

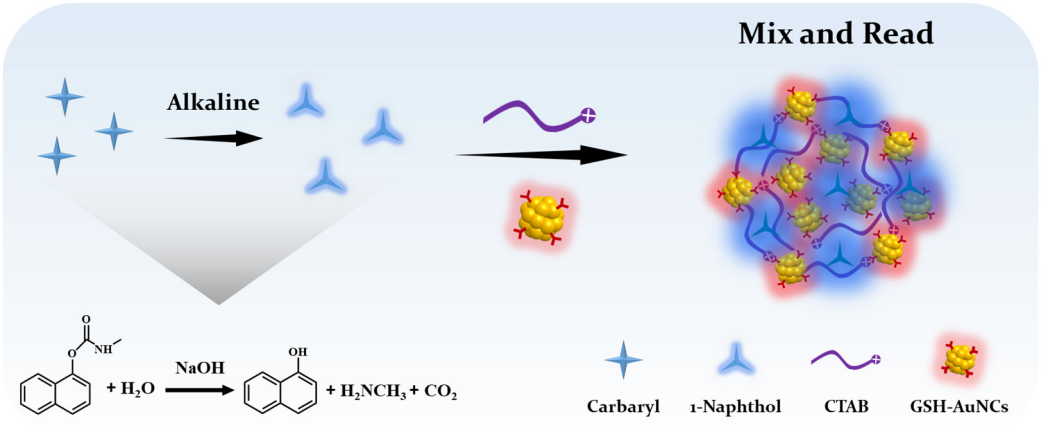

Figure 1. Schematic illustration of detection of carbaryl.

The AuNCs showed a quasi-spherical structure with an average size of 3.2 nm ± 0.6 nm (Figure 2A). In the high-resolution TEM images, the Au lattice spacing was determined to be 0.28 nm (Figure 2B); this represents the (1 1 1) crystal face of Au. As shown in Figure 2D, carbaryl (50 ng/mL) showed no fluorescence emission. Under the alkaline condition (10 mM NaOH), a weak emission peak appeared at 460 nm. The introduction of CTAB to the mixture resulted in the fluorescence emission peak at 460 nm blue-shifting to 450 nm, and emission of carbaryl hydrolysate increasing sharply, by 7-fold. In addition, under/mixing of carbaryl hydrolysate and CTAB, the fluorescence emission of GSH-Au NCs maintained stable under the same excitation wavelength. Thus, the GSH-Au NCs with red fluorescence emission can be used as a good reference for the blue fluorescence emission of carbaryl at 450 nm.

From the inserted photos in Figure 2, it can be seen that no obvious color change was observed in the carbaryl solution. However, dark and weak emission from the carbaryl solution with NaOH was observed under UV light. With the addition of CTAB, a bright blue emission from the mixture appeared. In the presence of red GSH-Au NCs, the emission from the mixture turned purple.

To further investigate the mechanism of the proposed method, UV-vis absorption spectra were measured for carbaryl and the hydrolysate. As can be seen in Figure 3, the carbaryl solution exhibited two absorption peaks (black curves) at 220 nm and 280 nm. After addition of NaOH, two absorption peaks (red curve) appeared at 245 nm and 330 nm, indicating that carbaryl was hydrolyzed into 1-naphthol under alkaline condition [22,23]. In the presence of CTAB, two absorption peaks at 245 nm and 330 nm red-shifted to 250 nm and 337 nm, respectively (blue curve), indicating that 1-naphthol was encapsulated into CTAB micelle [26]. This encapsulation of carbaryl hydrolysate could disperse the hydrophobic product, thus protecting it from aggregation and from water-molecule-induced fluorescence quenching. As a result, the intrinsic weak blue fluorescence of carbaryl was significantly enhanced. The surfactant Tween-20 also enhanced the fluorescence of carbaryl hydrolysis, although much more weakly than CTAB (Figure S1). In addition, the size distribution of the CTAB emulsion and the GSH-AuNCs were analyzed by DLS. As shown in Figure 3B–D, the mixture of the carbaryl hydrolysate emulsion and GSH-AuNCs was significantly larger than any other, indicating that a strong interaction existed between the carbaryl hydrolysate emulsion and the GSH-AuNCs.

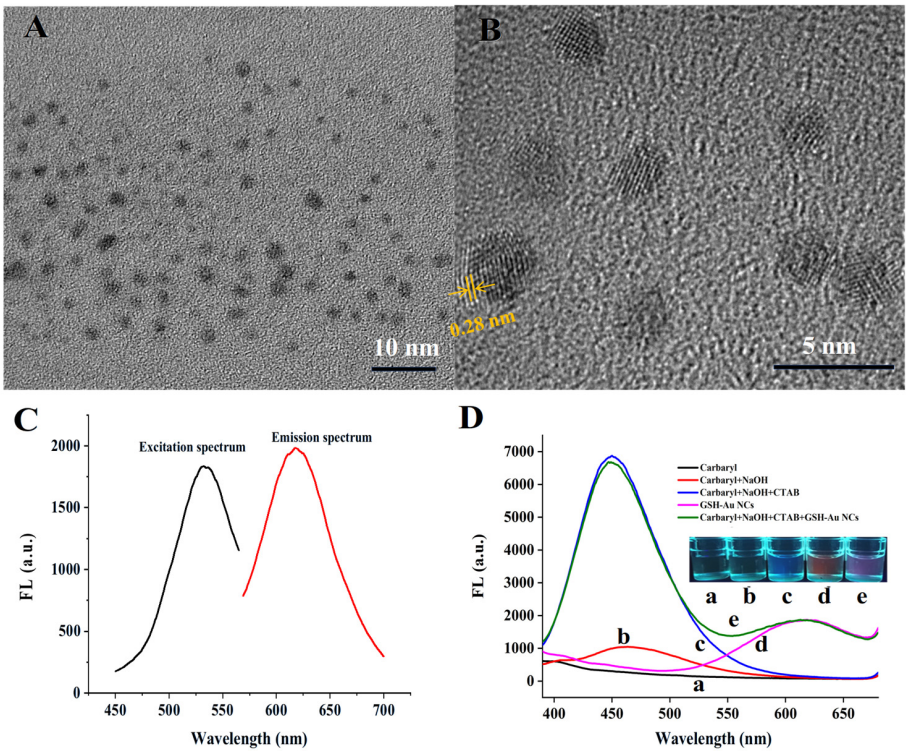

Figure 2. Characterization of GSH-AuNCs and feasibility of carboxyl fluorescent sensing. (**A**) Representative TEM image of GSH-AuNCs; (**B**) Latice spacing analysis of GSH-AuNCs; (**C**) Fluorescent of GSH-AuNCs; (**D**) Response of GSH-AuNCs to carboxyl hydrolysis. The insert image photos were obtained under UV light: a, carbaryl; b, carbaryl under alkaline hydrolysis; c, carbaryl hydrolysate with the presence of CTAB; d, GSH-AuNCs; e, carbaryl hydrolysate with the presence of CTAB and GSH-AuNCs.

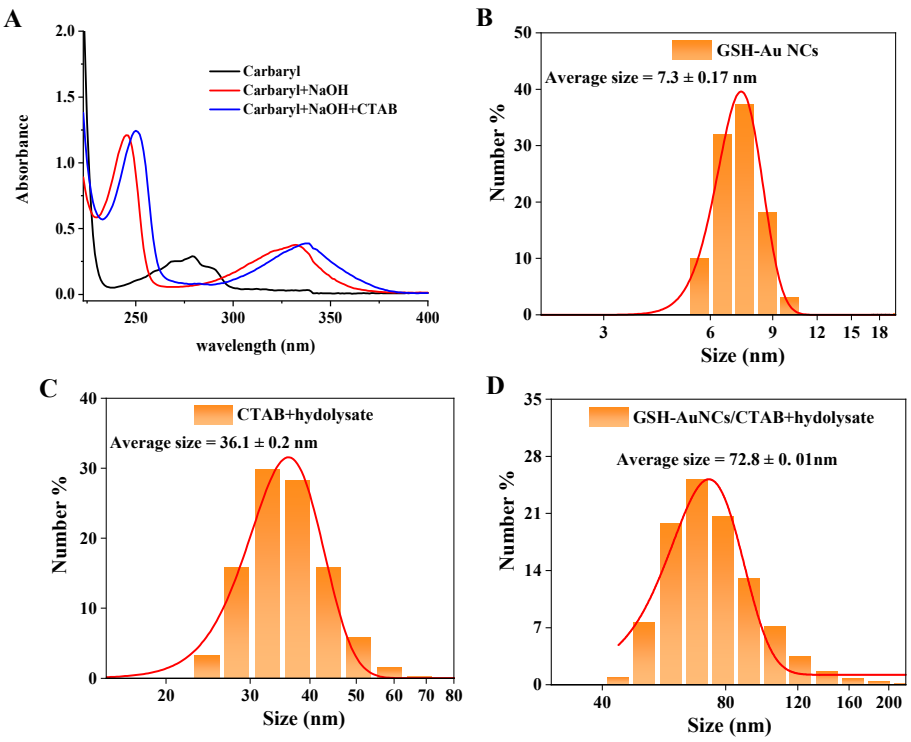

Figure 3. (**A**) UV-v is absorption spectra of carbaryl, carbaryl with NaOH and carbaryl with NaOH and CTAB. Size distributions of (**B**) GSH-AuNCs, (**C**) carbaryl hydrolysate emulsion, and (**D**) the mixture of GSH-AuNCs and carbaryl hydrolysate emulsion.

3.2. Optimization of Sensing Conditions

To achieve stable responses to the detection of carbaryl, the effects of the following experimental parameters were investigated: NaOH concentration, reaction temperature, CTAB concentration and hydrolysis time.

The effect of concentration of NaOH in a range of 1–20 mM on carbaryl sensing was investigated. As illustrated in Figure 4A, as NaOH concentration increased from 1 to 10 mM, a significant increase on the F_{450}/F_{620} value was observed (F_{450} and F_{620} are the fluorescence values at 450 nm and 620 nm, respectively). And the F_{450}/F_{620} value reached a plateau when the NaOH concentration was higher than 10 mM.

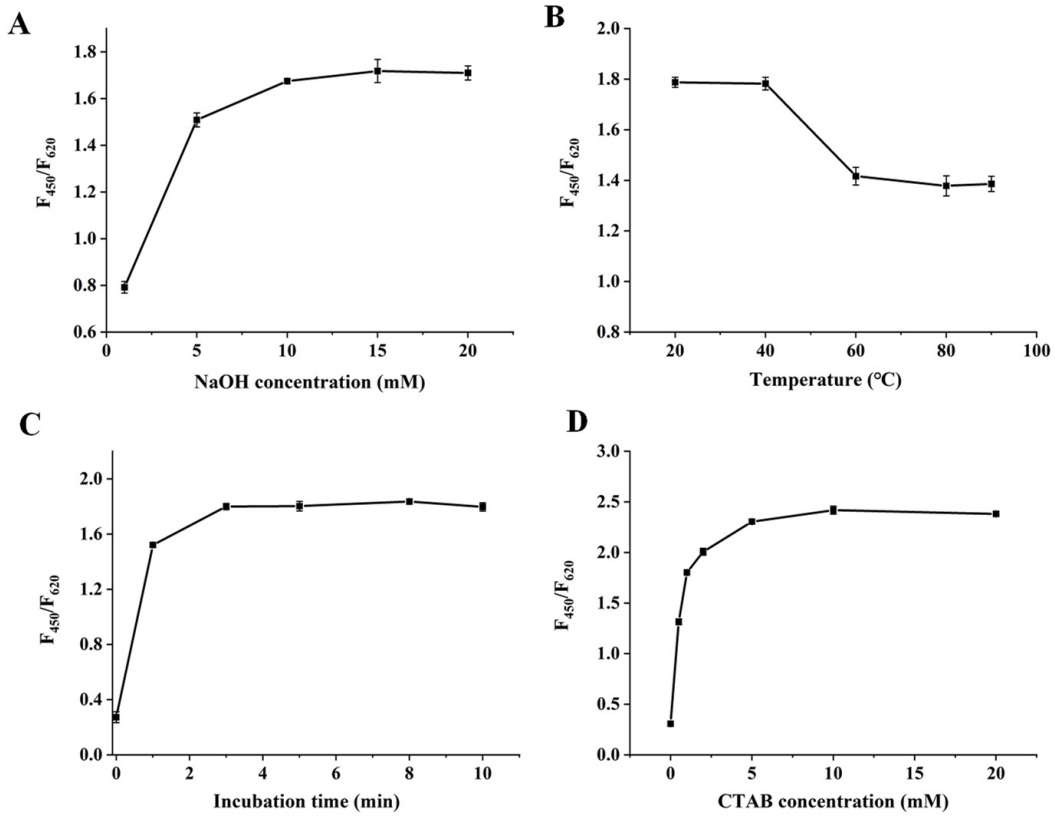

Figure 4. Effects of (**A**) NaOH concentration, (**B**) temperature, (**C**) incubation time and (**D**) CTAB concentration on the value of F_{450}/F_{620}. All experiments were repeated 3 times.

As shown in Figure 4B, the F_{450}/F_{620} value maintained a high level and remained stable in the 20 to 40 °C range, benefiting the ambient temperature operation. However, the signal obviously decreased as the temperature rose up to 60 °C, a finding likely due to the quenching of GSH-Au NCs to a certain extent.

To evaluate the effect of hydrolysis time on sensing responses, the carbaryl solution (30 ng/mL) was mixed with NaOH solution (10 mM) and then hydrolyzed at room temperature for 1, 3, 5, 8 or 10 min. As shown in Figure 4C, the hydrolysis reaction could be completed in 3 min, greatly benefiting the rapid detection of carbaryl.

Surfactants in aqueous solution can form micelle when they reach their particular critical micelle concentration; in this process, they carry out the functions of solubilization, sensitization, and stabilization in fluorescence detection [27]. Thus, the effect of CTAB concentration on the sensing response was investigated. As shown in Figure 4D, the fluorescence intensity at 450 nm was obviously enhanced, by nearly four-fold, at a concentration of 0.5 mM. As the CTAB concentration gradually increased to 20 mM, a seven-fold enhancement was achieved. The great fluorescence enhancement effect of CTAB on 1-naphthol should be due to the hydrophobic microenviroment for 1-naphthol provided by CTAB. This

condition can reduce collisions of electron clouds between 1-naphthol and water molecules, and protect the singlet state of the fluorescence emission.

Interestingly, with the GSH-Au NCs as reference signal, the F_{450}/F_{620} signal was enhance by nearly eight-fold at a much lower CTAB (5 mM) and a slightly higher was obtained at 10 mM (Figure 5B). These results were due to the slight quenching of GSH-Au NCs by CTAB after the GSH-Au NCs were absorbed onto the CTAB micelle surface. Thus, a lower-concentration CTAB (5 mM) could be selected as the optimal concentration; this may benefit the operation because too high a concentration of CTAB might easily produce air bubbles and disturb the solution blending operation.

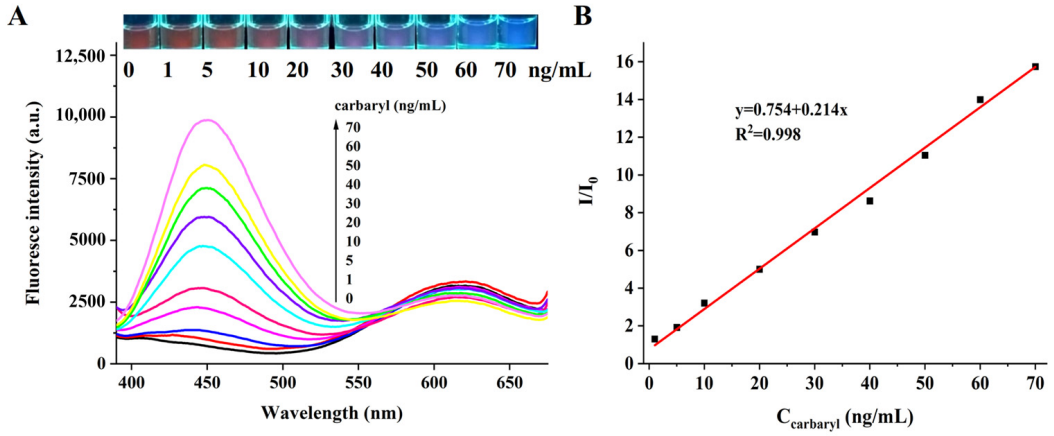

Figure 5. (**A**) Fluorescence spectra and photos obtained UV light of different carbaryl concentrations; (**B**) linear fitting curve for carbaryl detection.

3.3. Analytical Performance of Carbaryl Detection

As shown in Figure 6A, the blue fluorescence intensity gradually increased with the increased concentration of carbaryl in the range of 1 to 70 ng/mL. At the same time, the intensity of red fluorescence intensity exhibited a slow decrease.

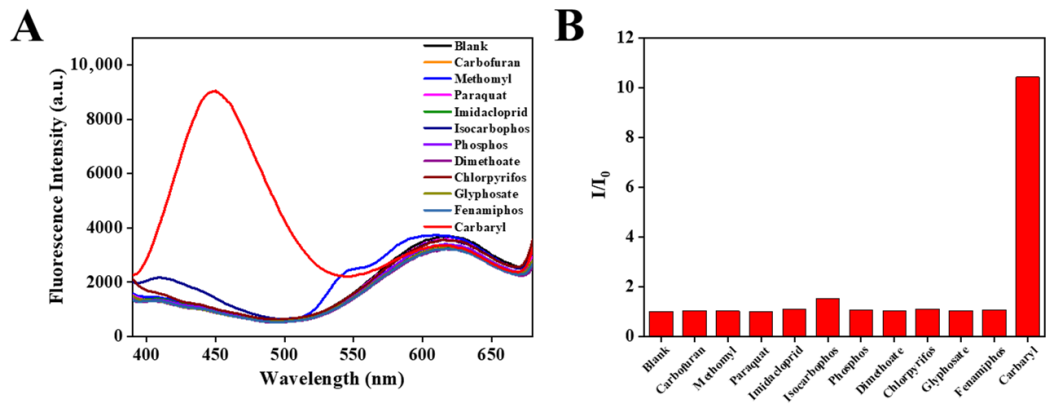

Figure 6. Specificity analysis of ratiometric detection of carbaryl. (**A**) Fluorescent spectra and (**B**) hitogram shows that the fluorescence response in the detection of different pesticides.

The photos inserted in Figure 5A show that with the increase in carbaryl concentration, the solution for ratiometric sensing demonstrated color changes from bright red to purple and, finally, to blue, all of which could be easily discriminated by the naked eye.

The fluorescence ratio signal at 450 nm to 620 nm (I/I_0) was used as a function of the concentration of carbaryl. As shown in Figure 5B, a linear equation, y = 0.214 x + 0.754 (R^2 = 0.998), was obtained for the range 1–70 ng/mL. The limit of detection (LOD) was

calculated to be 0.05 ng/mL based on 3σ/s (σ is the standard deviation of the blank value, and s is the slope of the equation).

Compared with some other typical fluorescence methods for the detection of carbaryl in recent years (Table 1), the proposed fluorescence detection of carbaryl based on intrinsic molecule fluorescence demonstrates ultrahigh sensitivity. Moreover, it is simple, enzyme-free, and involves a much shorter detection time.

Table 1. Comparison of several methods for detecting carbaryl.

Method	System	Principle	Signal Output	Linearity Range	LOD	Detection Time	Ref.
SERS	Surface-adsorbed nanosphere/AchE	AChE activity inhibition	/	/	0.47 ng/mL	40 min	[28]
Colorimetric	Ag@rGO	Aggregation/ Color reagents	/	0.025~12 μg/mL	13 ng/mL	15 min	[29]
Electro-chemistry	SWCNTs/PDDA/ AchE	AChE activity inhibition	/	1~1000 ng/mL	0.1 ng/mL	60 min	[30]
Electro-chemistry	Nile blue A/Carbaryl	Ratiometric/ Electrotransfer	/	2.5~18.5 μg/mL	0.25 μg/mL	10 min	[7]
Fluorescence	Phthalate-europium (Eu^{3+})/Diallyl phthalate	Complexation/ Fluorescence enhancement	Turn-on	0.06~2.50 μg/mL	2 ng/mL	10 min	[31]
Fluorescence	CdTe QDs/Carbaryl	Ratiometric fluorescence enhancement	Turn-on	0.05~14 μg/mL	0.12 ng/mL	5 min	[32]
Fluorescence	SiO_2@Gd_2O_3:Eu^{3+}@SiO_2 @MIP NPs	Fluorescence enhancement	Turn-on	16~80 μg/mL	10 μg/mL	20 min	[33]
Fluorescence	CQDs/AuNPs/AchE	IFE/AChE activity inhibition	Turn-on	0.2~150 μg/mL	0.06 ng/mL	45 min	[34]
Fluorescence	NH_2-MIL-101(Fe)/ o-phenylenediamine/ AchE	IFE/AChE activity inhibition	Turn-on	2~100 ng/mL	1.45 ng/mL	10 min	[35]
Fluorescence	GSH-AuNPs/CTAB	Ratiometric fluorescence enhancement	Turn-on	1~70 ng/mL	0.05 ng/mL	3 min	This method

According to previous reports, some other pesticides, such as organophosphorus also can also be hydrolyzed under alkaline condition. To evaluate the specificity of the proposed method, carbamate pesticides (carbofuran, methomyl), neonicotinoid pesticides (imidacloprid), organophosphorus pesticides (isocarbophos, phosalone, chlorpyrifos, dimethoate, glyphosate, fenamiphos) and paraquat at a 10-times-higher concentration (500 ng/mL) than carbaryl (50 ng/mL) were tested under the same condition. As shown in Figure 6, only carbaryl showed high fluorescence emission, when compared with all the other pesticides. Although the ammonium phosphine pesticide had an emission peak at 420 nm, its fluorescence intensity was much weaker than the carbaryl system. The above results demonstrate the high specificity of this fluorescent turn-on method for the detection of carbaryl.

3.4. Carbaryl Detection in Food Samples

The proposed method was further applied to detect carbaryl in spiked apple and cabbage. As shown in Table 2, the obtained recovery rates for detection in apple and cabbage samples were 90%~101% and 93%~110%, respectively, demonstrating that this method had great potential for use in detecting carbaryl in real samples.

Table 2. Detection of carbaryl in apple and cabbage samples (n = 3).

Sample	Spiked (ng/g)	Detected (ng/g)	Recovery (%)	RSD (%)
Apple	0	/	/	/
	4.0	3.6	90.0	8.6
	12.0	1.14	96.0	4.3
	24.0	2.42	101	2.7
Cabbage	0	/	/	4.8
	4.0	4.4	110	7.2
	12.0	12.6	105	5.3
	24.0	23.2	93	3.1

4. Conclusions

In summary, a fluorescent ratiometric carbaryl detection method was successfully constructed. We found that the intrinsic fluorescence of the carbaryl hydrolysate 1-naphthol could be greatly enhanced by CTAB. Integrating GSH-Au NCs with fluorescence-enhanced carbaryl hydrolysate emulsion, a ratiometric detection of carbaryl was successfully achieved. Intrinsic fluorescent enhancement detection was easily achieved with a mix-and-read detection mode. The method was also rapid (completed within 3 min) and ultra-highly sensitive. The feasibility of the proposed method was verified using real samples, and satisfactory results were obtained. In light of the abovementioned merits, we may say that this method has high potential in practical detection on carbaryl in foods.

Supplementary Materials: The following supporting information can be downloaded at: https://www.mdpi.com/article/10.3390/chemistry8030036/s1, Figure S1: Enhancement of Tween-20 on the carbaryl hydrolysis.

Author Contributions: X.C.: methodology, formal analysis, investigation, writing—original draft. J.J.: formal analysis, investigation, validation, writing—original draft. X.H.: data curation. C.P.: conceptualization, writing—review and editing, supervision, funding acquisition, project administration. All authors have read and agreed to the published version of the manuscript.

Funding: This work was supported by the National Key Research and Development Program (2022YFD2101105), the National Natural Science Foundation of China (31871879), and the Youth Engineering Project of Shandong Institute of Pomology (2024GSKY05).

Data Availability Statement: All data generated or analyzed during this study are included in this published article.

Conflicts of Interest: The authors have no competing interests to declare that are relevant to the content of this article.

References

1. Melchert, W.R.; Rocha, F. A greener and highly sensitive flow-based procedure for carbaryl determination exploiting long pathlength spectrophotometry and photochemical waste degradation. *Talanta* **2010**, *81*, 327–333. [CrossRef]
2. Chen, J.; Liu, Z.; Fang, J.; Wang, Y.; Cao, Y.; Xu, W.; Ma, Y.; Meng, X.; Wang, B. A turn-on fluorescence biosensor for sensitive detection of carbaryl using flavourzyme-stabilized gold nanoclusters. *LWT* **2022**, *157*, 113099. [CrossRef]
3. Sam-Ang, S.; Kraingkrai, P.; Watsaka, S.; Grudpan, K. A new method for spectrophotometric determination of carbaryl based on rubber tree bark peroxidase enzymatic reaction. *Microchem. J.* **2018**, *144*, 56–63. [CrossRef]
4. Dorozhko, E.V.; Gashevskay, A.S.; Korotkova, E.I.; Barek, J.; Vyskocil, V.; Eremin, S.A.; Galunin, E.V.; Saqib, M. A copper nanoparticle-based electrochemical immunosensor for carbaryl detection. *Talanta* **2021**, *228*, 122174. [CrossRef] [PubMed]
5. Indrajit, S.; Ajay, S.; Manjeet, A.; Khandal, R.K. Simultaneous Determination by Gas Chromatography of Lindane and Carbaryl in Combined Formulations. *J. Chem.* **2011**, *8*, 391–399. [CrossRef]

6. Nunes, G.S.; Marco, M.P.; Farré, M.; Barceló, D. Direct application of an enzyme-linked immunosorbent assay method for carbaryl determination in fruits and vegetables. Comparison with a liquid chromatography-postcolumn reaction fluorescence detection method. *Anal. Chim. Acta* **1999**, *387*, 245–253. [CrossRef]
7. Zhang, M.; Zhang, Z.; Yang, Y.; Zhang, Y.; Wang, Y.; Chen, X. Ratiometric Strategy for Electrochemical Sensing of Carbaryl Residue in Water and Vegetable Samples. *Sensors* **2020**, *20*, 1524. [CrossRef]
8. Wang, X.; Hou, T.; Dong, S.; Liu, X.; Li, F. Fluorescence biosensing strategy based on mercury ion-mediated DNA conformational switch and nicking enzyme-assisted cycling amplification for highly sensitive detection of carbamate pesticide. *Biosens. Bioelectron.* **2016**, *77*, 644–649. [CrossRef]
9. Korram, J.; Dewangan, L.; Nagwanshi, R.; Karbhal, I.; Ghosha, K.K.; Satnami, M.L. A carbon quantum dot–gold nanoparticle system as a probe for the inhibition and reactivation of acetylcholinesterase: Detection of pesticides. *N. J. Chem.* **2019**, *43*, 6874–6882. [CrossRef]
10. Huang, K.Y.; He, H.X.; He, S.B.; Zhang, X.-P.; Peng, H.-P.; Lin, Z.; Deng, H.-H.; Xia, X.-H.; Chen, W. Gold nanocluster-based fluorescence turn-off probe for sensing of doxorubicin by photoinduced electron transfer. *Sens. Actuators B Chem.* **2019**, *296*, 126656. [CrossRef]
11. Khaledian, S.; Noroozi-Aghideh, A.; Kahrizi, D.; Moradi, S.; Abdoli, M.; Ghasemalian, A.H.; Heidari, M.F. Rapid detection of diazinon as an organophosphorus poison in real samples using fluorescence carbon dots. *Inorg. Chem. Commun.* **2021**, *130*, 108676. [CrossRef]
12. Shen, Y.; Zhu, C.; Wei, Y.; Chen, H.; Wu, Z.; Ye, Y.; Han, D.-M. Engineering of Portable Smartphone Integrated with Liposome-Encapsulated Curcumin for Onsite Visual Ratiometric Fluorescence Imaging of Hypochlorite. *Chemistry* **2022**, *28*, e202200263. [CrossRef]
13. Liu, B.; Chen, W.; Dong, L.; Wang, T.; Pan, C.; Liu, D.; Wang, L.; Bai, R. Detection of trace levels of Pd^{2+} in pure water using a fluorescent probe assisted by surfactants. *Sens. Actuators B Chem.* **2016**, *237*, 899–904. [CrossRef]
14. Li, T.; Xie, L.; Long, R.; Tong, C.; Guo, Y.; Tong, X.; Shi, S.; Lin, Q. Cetyltrimethyl ammonium mediated enhancement of the red emission of carbon dots and an advanced method for fluorometric determination of iron(III). *Microchim. Acta* **2019**, *186*, 791. [CrossRef]
15. Du, G.; Mao, Y.; Abed, M.A.; Pu, L. Fluorescent Recognition of L- and D-Tryptophan in Water by Micelle Probes. *Mater. Chem. Front.* **2020**, *4*, 2384–2388. [CrossRef]
16. Oh, S.; Jeon, J.; Jeong, J.; Park, J.; Oh, E.-T.; Park, H.J.; Lee, K.-H. Fluorescent Detection of Methyl Mercury in Aqueous Solution and Live Cells Using Fluorescent Probe and Micelle Systems. *Anal. Chem.* **2020**, *92*, 4917–4925. [CrossRef]
17. Hu, X.; Liu, Y.; Duan, Y.; Han, J.; Li, Z.; Han, T. A turn-on type stimuli-responsive fluorescent dye with specific solvent effect: Implication for a new prototype of paper using water as the ink. *Spectrochim. Acta Part A Mol. Biomol. Spectrosc.* **2017**, *184*, 7–12. [CrossRef]
18. Li, X.; Yin, Y.; Deng, J.; Zhong, H.; Tang, J.; Chen, Z.; Yang, L.; Ma, L.-J. A solvent-dependent fluorescent detection method for Fe^{3+} and Hg^{2+} based on a rhodamine B derivative. *Talanta* **2016**, *154*, 329–334. [CrossRef]
19. Azath, I.A.; Pitchumani, K. Flavone modified-β-cyclodextrin as a highly selective and efficient fluorescent chemosensor for Cu^{2+} ions and l-histidine. *Sens. Actuators B Chem.* **2013**, *188*, 59–64. [CrossRef]
20. Tang, Q.; Wang, C.H.; Xi, Y.; Huang, Y.; Tao, Z. Host-Guest Complexes of l-Borneol with Cucurbituril and Cyclodextrin and Its Potential Use in Analysis of Drugs. *ChemistrySelect* **2019**, *4*, 6924–6929. [CrossRef]
21. Luo, Z.; Yuan, X.; Yu, Y.; Zhang, Q.; Leong, D.T.; Lee, J.Y.; Xie, J. From aggregation-induced emission of Au(I)-thiolate complexes to ultrabright Au(0)@Au(I)-thiolate core-shell nanoclusters. *J. Am. Chem. Soc.* **2012**, *134*, 16662–16670. [CrossRef]
22. Murillo Pulgarín, J.A.; García Bermejo, L.F.; Carrasquero Durán, A. Simultaneous chemiluminescent determination of carbaryl and 1-naphthol in soils using a flow-injection system. *Int. J. Environ. Anal. Chem.* **2018**, *98*, 111–123. [CrossRef]
23. Hawker, D. Kinetics of Carbaryl Hydrolysis: An Undergraduate Environmental Chemistry Laboratory. *J. Chem. Educ.* **2015**, *92*, 1531–1535. [CrossRef]
24. Wolfe, N.L.; Zepp, R.G. Carbaryl, propham and chlorpropham: A comparison of the rates of hydrolysis and photolysis with the rate of biolysis. *Water Res.* **1978**, *12*, 565–571. [CrossRef]
25. Fan, C.; Lv, X.; Liu, F.; Feng, L.; Liu, M.; Cai, Y.; Liu, H.; Wang, J.; Yang, Y.; Wang, H. Silver Nanoclusters Encapsulated into Metal-Organic Frameworks with Enhanced Fluorescence and Specific Ion Accumulation toward the Microdot Array-Based Fluorimetric Analysis of Copper in Blood. *ACS Sens.* **2018**, *3*, 441–450. [CrossRef] [PubMed]
26. Lu, C.; Cao, J.; Cheng, Y.; Jin, Y.; Qu, Y.; Xu, J. Fluorescence turn-on NapTp in CTAB micelles for efficient detecting ferric ions in aqueous system. *Sens. Actuators B. Chem.* **2018**, *255*, 3102–3107. [CrossRef]
27. Shi, Y.; Luo, H.Q.; Li, N.B. Determination of the critical premicelle concentration, first critical micelle concentration and second critical micelle concentration of surfactants by resonance Rayleigh scattering method without any probe. *Spectrochim. Acta Part A Mol. Biomol. Spectrosc.* **2011**, *78*, 1403–1407. [CrossRef]

28. Yamaguchi, U.; Ogawa, M.; Takei, H. Patterned Superhydrophobic SERS Substrates for Sample Pre-Concentration and Demonstration of Its Utility through Monitoring of Inhibitory Effects of Paraoxon and Carbaryl on AChE. *Molecules* **2020**, *25*, 2223. [CrossRef]
29. Phung, M.N.; Hoang, T.V.; Ngo, D.X.; Van Hoang, O.; Van Cuong, N.; Hop, D.T.B.; Tuan, T.Q.; Khi, N.T.; Huy, T.Q.; Le, A.-T. Reduced Graphene Oxide-wrapped Silver Nanoparticles for Applications to Ultrasensitive Colorimetric Detection of Cr (VI) Ions and Carbaryl pesticide. *New J. Chem.* **2020**, *44*, 7611–7620. [CrossRef]
30. Firdoz, S.; Ma, F.; Yue, X.; Dai, Z.; Kumar, A.; Jiang, B. A novel amperometric biosensor based on single walled carbon nanotubes with acetylcholine esterase for the detection of carbaryl pesticide in water. *Talanta* **2010**, *83*, 269–273. [CrossRef]
31. Xie, D.-D.; Han, R.-Y.; Shen, J.-C.; Xiao, C.-G.; Zheng, Z.-K.; Wang, Z.-W. Determination of Trace Carbaryl in Water Using Europium-Diallyl Phthalate as Fluorescent Probe. *Chin. J. Anal. Chem.* **2015**, *43*, 1069–1074. [CrossRef]
32. Shahdost-Fard, F.; Fahimi-Kashani, N.; Hormozi-Nezhad, M.R. A ratiometric fluorescence nanoprobe using CdTe QDs for fast detection of carbaryl insecticide in apple—ScienceDirect. *Talanta* **2021**, *221*, 121467. [CrossRef] [PubMed]
33. Long, Z.; Shen, S.; Lu, Y.; Lan, W.; Chen, J.; Qiu, H. Monodisperse core-shell-structured SiO_2@Gd_2O_3:Eu^{3+}@SiO_2@MIP nanospheres for specific identification and fluorescent determination of carbaryl in green tea. *Anal. Bioanal. Chem.* **2019**, *411*, 4221–4229. [CrossRef] [PubMed]
34. Chen, Y.; Qin, X.; Yuan, C.; Shi, R.; Wang, Y. Double responsive analysis of carbaryl pesticide based on carbon quantum dots and Au nanoparticles. *Dye. Pigment.* **2020**, *181*, 108529. [CrossRef]
35. Liu, P.; Li, X.; Xu, X.; Ye, K.; Wang, L.; Zhu, H.; Wang, M.; Niu, X. Integrating peroxidase-mimicking activity with photoluminescence into one framework structure for high-performance ratiometric fluorescent pesticide sensing. *Sens. Actuators B Chem.* **2021**, *328*, 129024. [CrossRef]